International Journal of Chronic Obstructive Pulmonary Disease

Dovepress
Taylor & Francis Group

Open Access Full Text Article

ORIGINAL RESEARCH

SCGB1A1 as a Key Regulator of Splenic Immune Dysfunction in COPD: Insights From a Murine Model

Xinye Chen[1,2,*], Qiujie Wang[3,4,*], Mingyan Gong[5], Yanru Wu[5], Xiaoping Huang[5], Fengzhan Ye[3,4], Linjie Huang[3,4], Shanping Jiang[3,4], Jianting Shi[3–5]

[1]Department of General Practice, Shenshan Medical Center, Memorial Hospital of Sun Yet-Sen University, Shanwei, People's Republic of China; [2]Department of General Practice, Sun Yat-Sen Memorial Hospital, Sun Yat-Sen University, Guangzhou, People's Republic of China; [3]Department of Respiratory and Critical Care Medicine, Sun Yat-Sen Memorial Hospital, Sun Yat-Sen University, Guangzhou, People's Republic of China; [4]Guangdong Provincial Key Laboratory of Malignant Tumor Epigenetics and Gene Regulation, Sun Yat-Sen Memorial Hospital, Sun Yat-Sen University, Guangzhou, People's Republic of China; [5]Department of Respiratory Medicine, Shenshan Medical Center, Memorial Hospital of Sun Yet-Sen University, Shanwei, People's Republic of China

*These authors contributed equally to this work

Correspondence: Shanping Jiang; Jianting Shi, Email jiangshp@mail.sysu.edu.cn; shijt5@mail.sysu.edu.cn

Introduction: Chronic Obstructive Pulmonary Disease (COPD) is a chronic inflammatory disorder characterized by irreversible airflow limitation and systemic immune impacts. COPD patients demonstrate an increased susceptibility to sepsis and septic shock, underscoring the importance of understanding its effects on splenic function.

Methods: A rat COPD model was established using lipopolysaccharide (LPS) and cigarette smoke exposure. Splenic function was assessed through carbon clearance assays, histological analysis, and high-throughput mRNA sequencing. In vitro assays were conducted to evaluate the role of secretoglobin family 1a member 1 (SCGB1A1) in macrophage activation and lymphocyte proliferation.

Results: Carbon clearance assays revealed a significant reduction in splenic phagocytic activity in the smoke-exposed group. Histological analysis showed lymphoid follicle atrophy and connective tissue hyperplasia. High-throughput mRNA sequencing identified 102 upregulated and 32 downregulated genes in the smoke-exposed group, with SCGB1A1 notably upregulated. In vitro assays confirmed that SCGB1A1 inhibits LPS-induced macrophage activation and Phytohemagglutinin (PHA)-induced lymphocyte proliferation.

Conclusion: These findings suggest that SCGB1A1 contributes to splenic immune dysfunction in COPD. Targeted inhibition of SCGB1A1 expression in the spleen may represent a potential therapeutic strategy to reduce the risk of sepsis in COPD patients.

Keywords: COPD, SCGB1A1, spleen, sepsis, macrophage

Introduction

Chronic obstructive pulmonary disease (COPD) is one of the most prevalent chronic diseases worldwide, characterized by irreversible airflow limitation, typically caused by prolonged exposure to harmful particles or gases, particularly tobacco smoke.[1] With the aging global population and increasing environmental pollution, the prevalence, disability rate, and mortality of COPD are rising year by year. The immunopathology of COPD stems from innate and adaptive immune responses triggered by chronic cigarette smoke exposure.[2] It is predominantly driven by intricate interactions between macrophages, dendritic cells, and lymphocytes, which initiate both cell-mediated and antibody-mediated inflammation.[3,4] This results in chronic airway remodeling, leading to irreversible airflow limitation and respiratory symptoms. Long-term inflammatory stimuli and structural changes in the airways significantly impact the local immune environment and immune cell status in the bronchopulmonary tissues of patients with COPD.[2] For instance, macrophages play a key role in regulating inflammation in COPD lungs by releasing various pro-inflammatory mediators, including matrix metalloproteinase (MMP)-12, cytokines, chemokines, and oxidants.[5–7] However, studies have shown that macrophages exhibit

Received: 20 November 2024
Accepted: 23 February 2025
Published: 3 March 2025

reduced phagocytic capacity following smoke exposure, which may contribute to the persistence of inflammation and hinder the clearance of pathogens and apoptotic cells.[8,9]

Inflammation in COPD occurs both at the pulmonary and systemic levels. Serum biomarkers such as cytokines, adipokines, C-reactive protein (CRP), and coagulation factors are elevated in both the stable phase and during exacerbations.[10,11] The systemic manifestations of COPD are largely driven by this inflammatory response, highlighting the disease's organ-specific and systemic effects.[12] Notably, COPD affects not only the local immune system in the lungs but also has a significant impact on the systemic immune system, particularly the lymphocytes and monocyte-macrophage system. Flow cytometric analyses of peripheral blood by Freeman et al demonstrated a significant reduction in CD4+ and CD8+ T cells during acute exacerbation of COPD, both in absolute numbers and as a percentage of total leukocytes, which may compromise systemic immune surveillance and the ability to defend against viral infections.[13] Another study reported that blood monocytes in patients with severe COPD exhibit unexpected pre-differentiation, predominantly characteristic of M2 macrophage polarization, leading to the emergence of an unusual M2-like monocyte population with elevated CCR5 expression.[14] These findings suggest that circulating monocytes in severe COPD may have a cellular phenotype that allows for increased mobilization and reduced phagocytic activity.[14,15] Moreover, multiple studies have shown that patients with COPD face a significantly increased risk of developing sepsis or septic shock following invasive surgeries or procedures, suggesting a marked impairment in pathogen clearance and immune competence in peripheral blood.[16–18]

The spleen plays a crucial role in the immune system by filtering blood through its network of macrophages, which phagocytose and eliminate bloodborne pathogens. Splenic B and T cells contribute to antibody production and the formation of immune memory, essential for long-term immune protection and response to reinfection.[19,20] Additionally, the spleen produces cytokines and chemokines that regulate immune responses, which are critical in preventing systemic infections and sepsis.[20,21] Splenectomy has shown therapeutic benefits in conditions like sickle cell anemia, thalassemia, idiopathic thrombocytopenic purpura (ITP), Hodgkin's disease, and various lymphomas. However, the procedure increases infection risk and may trigger overwhelming post-splenectomy infection (OPSI), a severe form of sepsis with a high mortality rate.[22–24]

Given the substantial evidence supporting impaired pathogen clearance and immune function in the peripheral blood of COPD patients, and the spleen's critical role in sepsis immunity, we hypothesize that COPD may lead to compromised splenic immune function. In this study, we constructed a rat COPD model using cigarette smoke exposure. For the first time, we systematically examined the mRNA profiling of spleen in the context of COPD, identified key molecular players, and explored the underlying mechanisms at the molecular level, thereby providing novel insights into the systemic immune effects of COPD.

Materials and Methods

Animals

Male SD rats aged 6–8 weeks and weighed between 230–270 grams were obtained from Guangdong Medical Laboratory Animal Center. All the experiments were performed in accordance with the protocol approved by the Institutional Animal Care and Use Committee at the Medical College of Sun Yat-sen University (Approval Number: SYSU-IACUC-2019-000180), following the guidelines outlined in the "Laboratory Animal Welfare and Ethical Review Guidelines" (GB/T 35892-2018) issued by the Standardization Administration of the People's Republic of China.

Establishment of Rat Models with Chronic Obstructive Pulmonary Disease

A total of 20 specific pathogen free (SPF) SD rats were used in this study. Rats were initially allowed to acclimate for one week and were randomly divided into two groups with ten rats in each group: the control group and the smoke-exposed group. Rats in the smoke-exposed group were anesthetized on the 1st and the 15th day, and an incision was made to expose the trachea for intratracheal instillation of LPS (200 μg/200 μL, Sigma, United States). Rats were then exposed to cigarette smoke (Daqianmen cigarettes, Shanghai tobacco group company, China). Exposure to cigarette smoke was performed in a 60 cm × 60 cm × 70 cm closed glass box for 30 min twice daily, starting from the 2nd day to the 14th day

and from the 16th to the 30th day. Rats in the control group received intratracheal instillation of sterilized normal saline and were left to breathe in a glass box of normal air. General conditions and statuses of all rats were observed and the weights were taken every day. The rats were sacrificed on day 31.

Hematoxylin-Eosin (HE) Staining

The lung and spleen tissues were paraformaldehyde, embedded in paraffin and cut into 4 μm thick slices. All sections were dewaxed with xylene and hydrated with ethanol. Sections were stained by hematoxylin and counter-stained by eosin. The samples were observed under a light microscope and the images were captured.

Carbon Clearance Test

The experiment was performed following established methods.[25] In accordance with the aforementioned protocol, rats were divided into two groups and treated accordingly for 30 days. On day 31, both groups were administered 10 mL/kg of carbon ink suspension (Ankur Minerals Pvt. Ltd., India), diluted with eight parts saline, via intravenous injection through the tail vein. Blood samples were collected at 5 and 15 minutes post-injection. To measure optical density, 25 μL of the collected blood was mixed with 3 mL of 0.1% sodium carbonate, and absorbance was measured at 675 nm. The carbon clearance rate was calculated using the formula: $k = (\text{In OD1} - \text{In OD2})/(t2 - t1)$.

RNA-Seq Data Processing of Rat Spleen Tissues

Total RNA from spleen tissues of the control group and the smoke-exposed group was isolated using TRIzol (Invitrogen, United States), and purified with the RNeasy mini kit (QIAGEN, Germany) according to the manufacturer's instructions. Poly-A selection and cDNA synthesis were performed using TruSeq Stranded mRNA kit (Illumina, United States). After PCR amplification, the sequencing was done on DNBSEQ platform (BGI Group, China). This project used the filtering software SOAPnuke developed by BGI independently for filtering. After quality control, the filtered clean reads were aligned to the reference sequence using the HISAT software, a fast and memory-efficient tool developed by the University of Maryland. Then, the statistics of the mapping rate and the distribution of reads on the reference sequence are used to evaluate the second quality control. Quantitative gene analysis based on gene expression was performed.

Identification of DEGs

The NetworkAnalyst online tool (https://www.networkanalyst.ca) was utilized to identify the differentially expressed genes (DEGs) between samples from rats in the control group and the smoke-exposed group. Data normalization was performed using the log2-counts per million (logCPM) transformation method. Statistical analysis was conducted using EdgeR, with all other parameters set to default settings. DEGs were defined as genes with an adjusted P-value (adj. P) less than 0.05 and a |log Fold Change| (|log FC|) greater than 1.0. Genes with a log FC greater than 1.0 were classified as up-regulated, while those with a log FC less than −1.0 were classified as down-regulated.

RT-qPCR

RNA extraction was conducted using TRIzol reagent (TAKARA, Japan). The purity and concentration of the extracted RNA were determined using the NanoDrop One Spectrophotometer (Thermo Fisher Scientific, United States). Subsequently, 500 ng of RNA was employed for reverse transcription reactions, followed by quantitative polymerase chain reaction using the LightCycler FastStart DNA Master SYBR Green I kit (TAKARA, Japan) and the Roche 480 PCR machine (Roche, Switzerland). The housekeeping genes GAPDH and U6 were utilized as internal controls.

Western Blot

Total protein was extracted using RIPA lysis buffer (Epizyme, China) and quantified with a BCA protein quantification kit (Epizyme, China) following the manufacturer's instructions. The protein samples were mixed with 5× loading buffer (Epizyme, China), boiled at 98°C for 10 minutes, and then stored at −80°C. Subsequently, the protein samples were separated on 10% SDS-PAGE gels at 120 mV for 30 minutes and transferred onto polyvinylidene difluoride (PVDF) membranes (Millipore, United States) using electroblotting at 250 mA for 90 minutes. The membranes were blocked with

5% non-fat powdered milk in 0.1% TBST solution at room temperature for 1 hour, followed by overnight incubation at 4°C with primary antibodies: SCGB1A1 (1:1000, Abcam, UK) and β-actin (1:1000, CST, United States). HRP-labeled IgG (Beyotime, China) was used as the secondary antibody, and chemiluminescent substrate reagent (Epizyme, United States) was used for detection. The intensity of the Western Blot bands was quantified using the ImageJ software (National Institutes of Health, United States). The results were normalized to the loading control (β-actin) to ensure consistency across samples.

Enrichment Analysis of Pathways and Biological Processes

To elucidate the biological implications of the studied genes, we employed the Metascape platform (https://metascape.org) for comprehensive enrichment analysis. This approach facilitated the interpretation of gene functions within their biological frameworks. Enrichment assessments of the DEGs were systematically conducted through various databases, including the Gene Ontology (GO) Biological Processes, Kyoto Encyclopedia of Genes and Genomes (KEGG) Pathways, Reactome Gene Sets and WikiPathways, utilizing Metascape.

Gene Set Enrichment Analysis

Enrichment analysis of gene sets (GSEA) was carried out through WebGestalt tools (http://www.webgestalt.org). This method involves categorizing genes by their expression disparities across two sample sets, correlating these findings with established gene sets across the entire genome. WebGestalt automatically excludes gene sets comprising fewer than five or exceeding 2000 genes in this analysis. KEGG pathway and GO biological processes functional database were utilized for GSEA analysis by WebGestalt.

Cell Culture and Stimulation

We further investigated the influence of SCGB1A1 protein on the responsiveness of lymphocytes and macrophages to inflammatory stimuli in vitro. Rat spleen lymphocytes and peritoneal macrophages, obtained from Wuhan Pricella Biotechnology Co., Ltd. (China), were cultured in RPMI 1640 medium enriched with 10% FBS and 1% penicillin/streptomycin. Cells were incubated at 37°C in a 5% CO_2 humidified atmosphere. Both cell types were seeded at a density of 1×10^5 cells per well in 12-well plates, set up in triplicate. They were treated with lipopolysaccharide (LPS, 1 μg/mL from Invivogen) or phytohemagglutinin (PHA, 10 μg/mL from Sigma), either with or without 5 μg/mL recombinant SCGB1a1 protein (Creative BioMart, United States). After 72 hours of stimulation, culture supernatants were harvested for cytokine analysis using enzyme-linked immunosorbent assay (ELISA). Lymphocyte proliferation was analyzed using a WST-8 Cell Counting Kit-8 (Beyotime, China) according to the manufacturer's protocol.

ELISA Analysis

Culture supernatants were collected to measure the concentration of IL-1β, TNF-α, or IL-2 with commercially available ELISA kits (BD biosciences, United States) according to the manufacturer's protocol. Multi-function enzyme spectrometer was used to detect the absorbance at 450nm.

Statistical Analysis

Data were analyzed by GraphPad Prism version 10 (GraphPad Software, United States). Results were expressed as mean ±s.e.m. The Student's *t*-test, one-way analysis of variance and Tukey multiple comparison tests were adopted. Two-sided P-values were subject to a significance level of 5%.

Results

Establishment and Validation of the Rat Model

In this study, we have developed a rat model of chronic obstructive pulmonary disease established by cigarette smoking exposure combined with airway instillation of bacterial LPS (Figure 1A). In the smoke-exposed group, the rats exhibited a reduced diet intake, slow response, rapid and shallow breathing, dry hair, and constant loss of the body weight (Figure 1B and C). Judging from the gross appearance change of the lung tissues of smoke-exposed rats, the lung volume

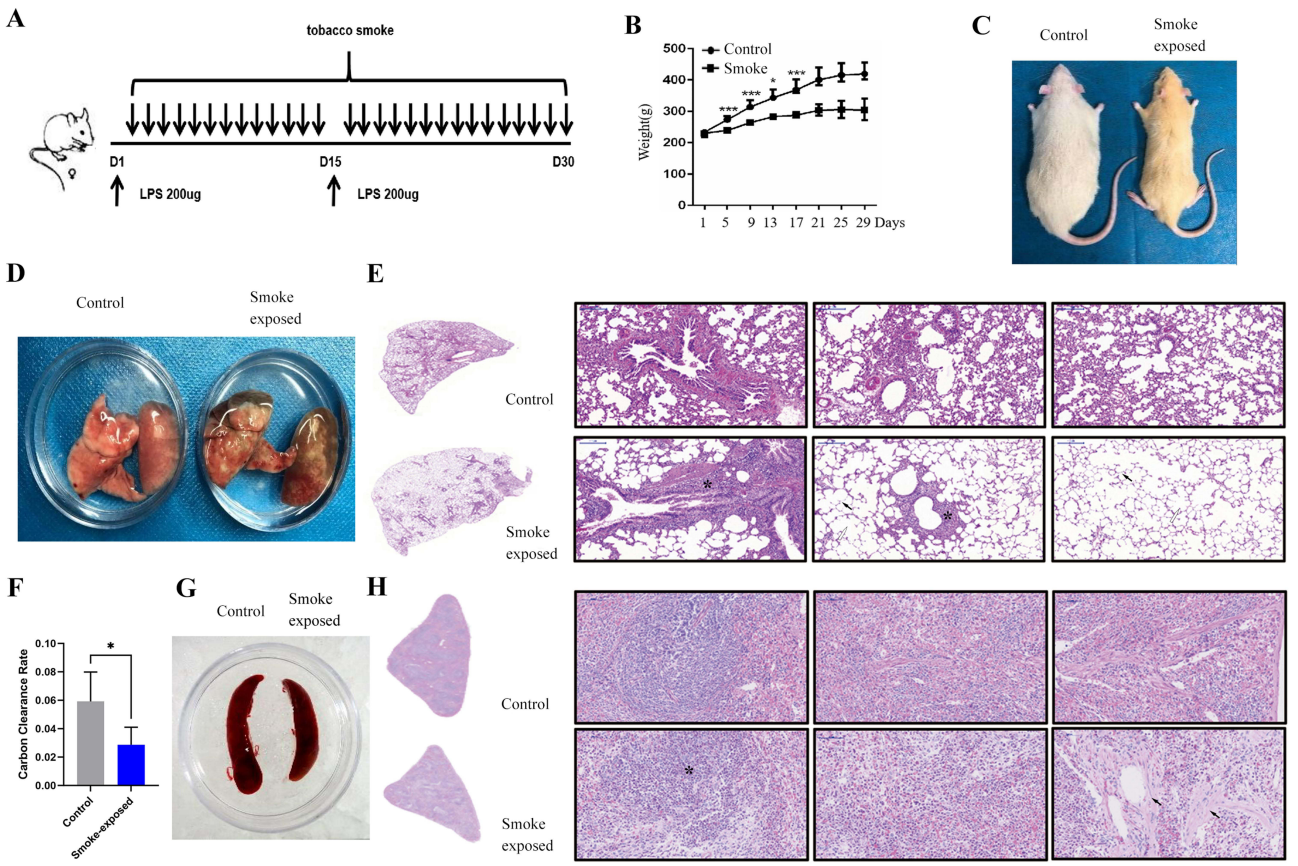

Figure 1 Development of COPD Rat Model and Histopathological Findings of Lung and Spleen Tissues. (**A**) The rat model of COPD established by cigarette smoking exposure combined with airway instillation of bacterial LPS. Timeline of the experimental protocol. (**B**) Weight of the rats from control and smoke-exposed group. Mean±s.d., n=10, *p<0.05, ***p<0.001 vs control group. (**C**) Representative images of SD rats (left-Control group; right-Smoke-exposed group). (**D**) Representative images of lungs (left-Control group; right-Smoke-exposed group). (**E**) Morphological manifestations of lung tissues of rats. Representative images of H&E staining of rat lung sections as shown at a magnification of ×100. Thickened bronchial wall, increased infiltrated inflammatory cells in the airway (*), filmy alveolar wall (black arrow), partial alveolar fusion, and pulmonary bullae (white arrow) were seen in rats from smoke-exposed group. (**F**) Splenic phagocytosis in rats analyzed by carbon clearance assay. Mean±s.d., n=4, *p<0.05 vs control group. (**G**) Representative images of SD rats, lungs and spleen (left-Control group; right-Smoke-exposed group). (**H**) Representative images of H&E staining of rat spleen sections as shown at a magnification of × 100. Atrophied lymphoid follicles (*) and fibrous connective tissue hyperplasia (black arrow) were observed in spleen tissues of rats in smoke-exposed group. A portion of the images in this figure was previously published in a non-SCI Chinese journal [Wang Q, et al. Lingnan Journal of Emergency Medicine, 2020, 25(05): 442–447] and is reproduced here with permission.

was increased along with grayish brown materials deposition (Figure 1D). Images of lung tissues of the smoke-exposed rats stained with H&E showed the thickened bronchial wall, necrosis and exfoliation of bronchial epithelial cells, and increased infiltrated inflammatory cells in the airway (Figure 1E). Filmy alveolar wall, and pulmonary bullae were also seen in rats from smoke-exposed group (Figure 1E).

Alterations in Splenic Phagocytic Function and Histology

The immune function of the spleen is primarily reflected in its ability to clear pathogens from peripheral blood. To assess splenic function, we conducted a carbon clearance test. The results showed that the carbon clearance rate in the smoke-exposed group was significantly reduced compared to the control group ($P<0.05$), indicating that smoke exposure can lead to a marked impairment of splenic immune function (Figure 1F). Rat spleen lymphocytes may play an important role in the pathogenesis of COPD and we further focused on the morphologic changes of spleen tissues. The length of spleen tissues of the smoke-exposed rats was shortened by appearances (Figure 1G). Compared with the control group, lymphoid follicles in spleen tissues of rats in smoke-exposed group were atrophied, and fibrous connective tissue hyperplasia was observed in images of H&E staining (Figure 1H).

https://doi.org/10.2147/COPD.S506332

Analysis and Validation of Sequencing Data

The gene expression matrix of mRNA sequencing results from spleen tissue of smoke-exposed and control group rats is provided in Supplementary Table 1 of this article. To evaluate the DEGs, we utilized the NetworkAnalyst online tool to analyze our sequencing data, which comprised 6 tissue samples (3 samples for each group). Figure 2A exhibits a volcano plot depicting all genes in the smoke-exposed group compared to the control group. In total, 134 DEGs were identified after filtration, as their |logFC| was greater than 1.0 and the adjusted P-value was less than 0.05 in samples from the smoke-exposed group compared to the control group. Among these DEGs, 102 genes were up-regulated, outnumbering the 32 down-regulated genes. The volcano plot visually portrays the distribution of all genes based on fold change and

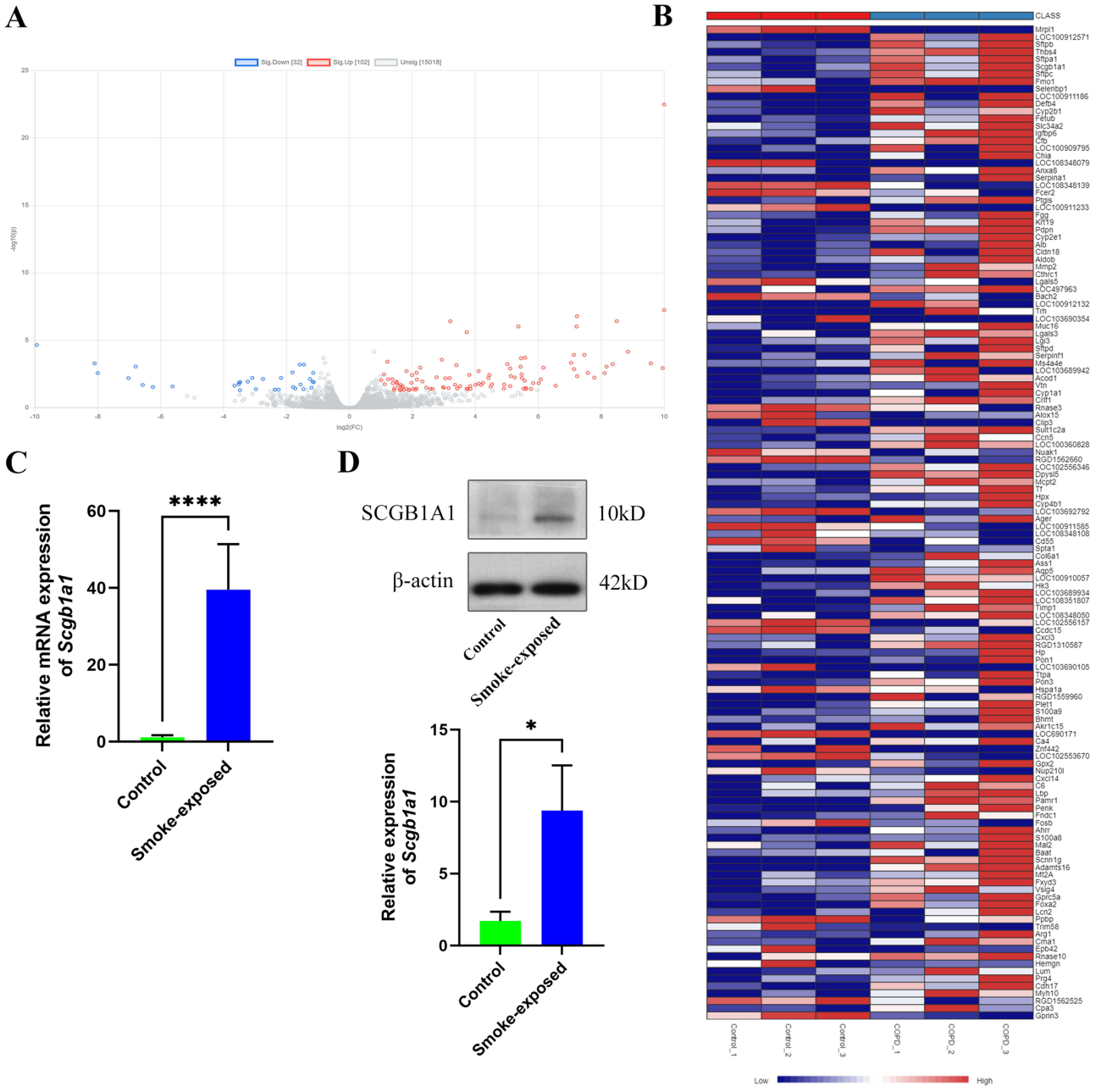

Figure 2 Gene Expression in the Spleen of Rats from Smoke-exposed (COPD) and Control Groups. (**A**) Volcano plots showing significantly up-regulated (red) and down-regulated (blue) genes (|logFC| >1.0, adjusted p-value <0.05); (**B**) Heat map showing the upregulated (red) and downregulated (blue) DEGs in these samples; (**C**) Expression of Scgb1a1 in the spleen from control and smoke-exposed rats, assessed by RT-qPCR. (n=6, ****p < 0.0001 vs control group) (**D**) Representative Western blot image showing SCGB1A1 expression in rat spleen tissue, along with the quantitative analysis result. (n=3, *p < 0.05 vs control group).

P-value. Blue, red, and grey points denote down-regulated, up-regulated, and non-regulated genes, respectively. The heat map representing the filtered DEGs is presented in Figure 2B.

Upon comprehensive analysis of the top five significant up-regulated DEGs ranked by -log10(P), we discovered that *Scgb1a1* (protein name secretoglobin 1A1, SCGB1A1) is closely associated with COPD and immune response, even though existing literature indicates that the SCGB1A1 protein is commonly expressed in the lung and reproductive system. We further validated the expression of SCGB1A1 in spleen tissue using RT-qPCR and Western blot. Our results revealed a significant up-regulation of SCGB1A1 in the spleen tissues of rats exposed to smoke at both mRNA and protein levels compared to the control group (Figure 2C and D).

Enrichment Analysis

We performed enrichment analysis of GO biological processes, KEGG pathways, Reactome gene sets, and WikiPathways using Metascape to investigate the biological changes occurring in the spleens of rats exposed to smoke. Figure 3A indicates that the up-regulated genes were significantly enriched in processes related to the response to LPS, oxygen levels, acute-phase response, regulation of toll-like receptors (TLRs) by endogenous ligands, tissue remodeling, and negative regulation of cytokine production. Conversely, down-regulated genes showed a notable enrichment in the regulation of protein polymerization, T cell proliferation, and adaptive immune response (Figure 3B). GSEA conducted via WebGestalt yielded slightly different findings (Figure 3C and D). Given our study's focus on immune responses within the spleen, enrichment plots of response to IL-6 (NES=2.19, FDR<0.01) and TCR signaling pathway (NES=−1.52, FDR=0.66) have been specifically highlighted in Figure 3E and F.

Effects of SCGB1A1 on the Activation of Macrophages and Lymphocytes

To further validate the effects of SCGB1A1 on immune cells at the cellular experiment level, we introduced SCGB1A1 to activated macrophages and lymphocytes in vitro. By assessing the secretion of characteristic cytokines, we clarified the impact of SCGB1A1 on the activation of macrophages and lymphocytes. Figure 4A shows that SCGB1A1 treatment did not significantly alter IL-1β levels in macrophages compared to untreated controls. In contrast, IL-1β release was significantly elevated in macrophages stimulated with LPS, but this was substantially reduced by SCGB1A1 supplementation. Specifically, macrophages treated with LPS and SCGB1A1 exhibited significantly lower IL-1β levels than those treated with LPS alone ($P<0.05$). SCGB1A1 also consistently reduced TNF-α release in LPS-stimulated macrophages (Figure 4A). However, SCGB1A1 did not significantly affect IL-2 release from PHA-activated lymphocytes as shown in Figure 4B ($P\geq0.05$).

SCGB1A1 Inhibited PHA-Induced Proliferation of Lymphocytes

Results of enrichment analysis indicate that lymphocyte proliferation is inhibited in the spleen of rats exposed to smoke. To evaluate the impact of SCGB1A1 on lymphocyte proliferation, we analyzed both unstimulated and activated lymphocytes. SCGB1A1 significantly reduced PHA-induced lymphocyte proliferation at a concentration of 5 μg/mL ($P<0.05$). However, it had no effect on the proliferation of unstimulated lymphocytes (Figure 4C).

Discussion

Secretoglobin family 1a member 1 (SCGB1A1), also known as club cell secretory protein (CCSP), is a member of the secretoglobin protein family, predominantly secreted by club cells located in the airway epithelium of the terminal bronchioles.[26] Due to its 16 kDa molecular weight, it is also referred to as CC16. Over time, it has been given several other names, including Clara Cell Secretory Protein, uteroglobin, CC10, CC17, and urine protein 1.[27] Under physiological conditions, SCGB1A1 is abundantly present in the lungs and is also detectable in both blood and urine.[26,28,29] Obstructive lung diseases are often associated with reduced levels of SCGB1A1, possibly due to diminished production or loss of club cells.[30,31] On the other hand, elevated SCGB1A1 levels have been observed in several restrictive lung diseases, both in the lungs and circulation, likely resulting from club cell dysfunction and increased lung permeability.[32–35] Recent research highlights the multiple pathways through which SCGB1A1 attenuates both acute and chronic lung inflammation, positioning it as a promising therapeutic target for inflammatory lung conditions.[36–38]

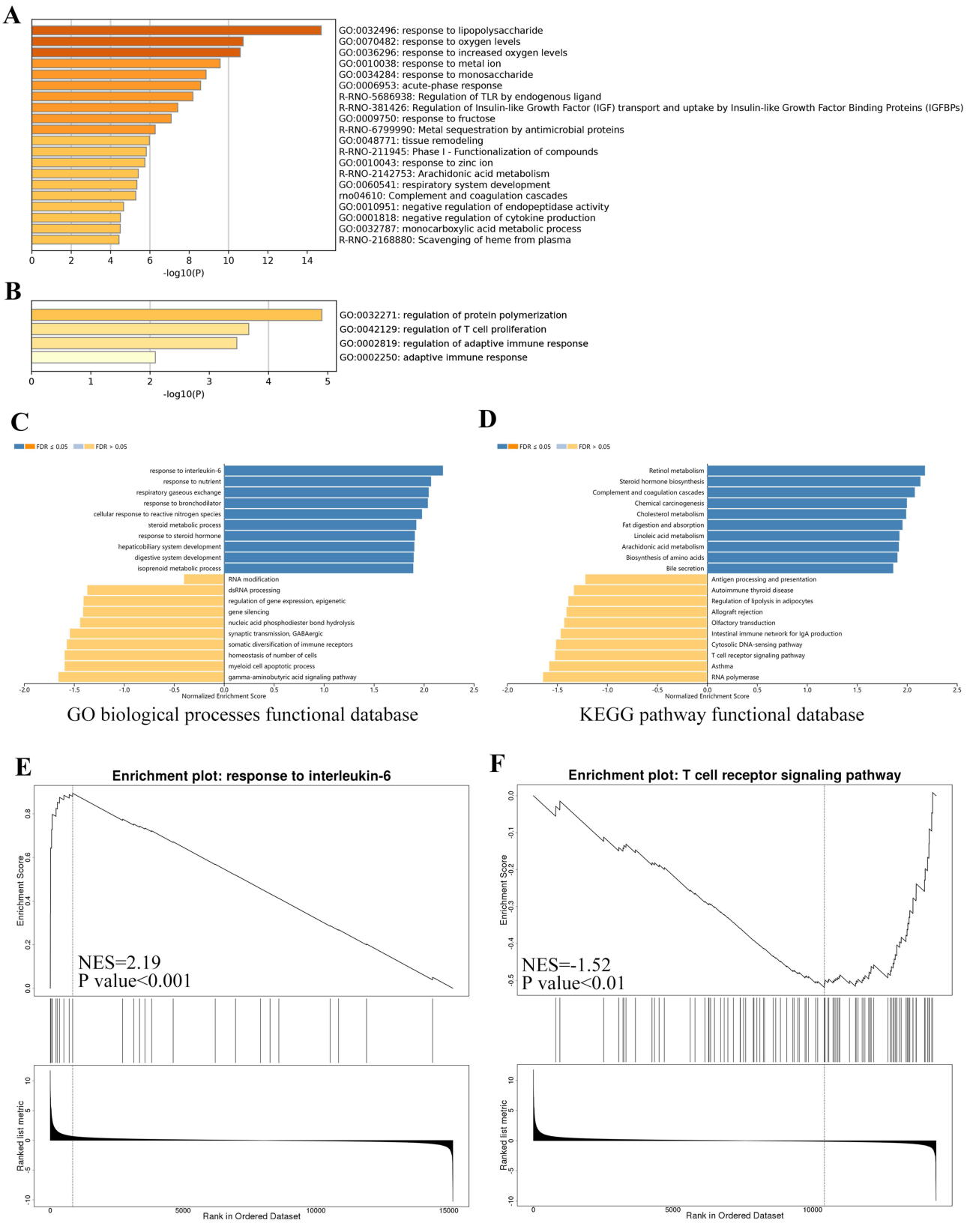

Figure 3 Functional Enrichment of Pathways and Biological Processes. (**A**) Bar graph depicting the enriched terms among the up-regulated genes, highlighting the top 20 biological pathways ranked by p-value and the proportion of genes involved. (**B**) Bar graph showing enriched terms among the down-regulated genes, featuring 4 biological pathways characterized by p-values (<0.01) and the percentage of genes involved. (**C**) Results of GSEA on the GO database for biological processes, identifying 10 positively associated categories and 10 negatively associated categories as enriched, all displayed in the bar chart. (**D**) Outcomes of gene set enrichment analysis on the KEGG pathway functional database. (**E**) GSEA enrichment plot illustrating the correlation between genes in the IL-6 response gene set and smoke-exposure. (**F**) GSEA enrichment plot demonstrating the correlation between genes in the T cell receptor signaling pathway gene set and smoke-exposure.

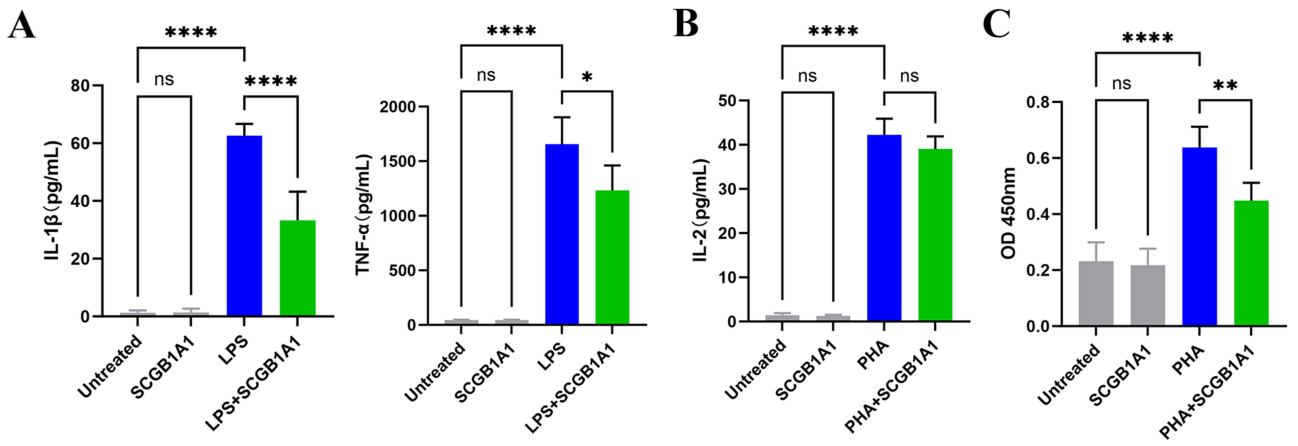

Figure 4 Effects of SCGB1A1 on Macrophages and Lymphocytes. (**A**) Release of IL-1β and TNF-α from purified macrophages in response to LPS, both with and without the addition of recombinant SCGB1A1 protein. (**B**) Release of IL-2 from purified lymphocytes stimulated by PHA, conducted in the presence and absence of recombinant SCGB1A1 protein. (**C**) Optical density (OD) at 450 nm from CCK-8 assays, indicating lymphocyte proliferation in response to PHA with and without recombinant SCGB1A1 protein. Data from four biological replicates are plotted as mean±SEM, ****P<0.0001, **P<0.01, *P<0.05, ns: P≥0.05.

SCGB1A1 has been shown to be closely linked to COPD. Studies have identified deficits in SCGB1A1 among COPD patients. Smokers with COPD have lower serum levels of SCGB1A1 compared to smokers without airflow limitation, and a negative correlation between SCGB1A1 levels and disease severity has been reported.[30,31,39] Furthermore, lower SCGB1A1 levels are associated with a faster decline in FEV1, not only in COPD patients but also in the general adult population.[40,41] Recent studies have highlighted that childhood SCGB1A1 deficits may predict impaired lung function in adolescence and adulthood.[31,39] These findings suggest a protective role for SCGB1A1 in COPD, potentially due to its regulatory effects on innate and adaptive immune responses, which mitigate pulmonary inflammation in both acute and chronic lung injuries. For example, a study conducted at the University of Montpellier demonstrated that recombinant human SCGB1A1 (rhSCGB1A1) reduced neutrophil chemotaxis in COPD airway epithelia by neutralizing IL-8.[42] This interaction was validated through several methods, with higher SCGB1A1/IL-8 ratios being linked to reduced neutrophil infiltration in COPD patients.[42] Contrary to these existing findings, our study discovered a significant increase in SCGB1A1 expression in the spleen of COPD model rats, suggesting its potential role as a key factor in splenic immune dysfunction. This observation indicates that SCGB1A1 may exhibit tissue-specific expression differences in COPD and could act not solely as a protective agent but potentially as a "double-edged sword" in disease progression. However, the conclusion that SCGB1A1 regulates splenic immune function is largely based on indirect inferences, and it is not robust enough until validated by well-designed animal intervention studies, such as using *Scgb1a1*-deficient mice.

SCGB1A1 is predominantly expressed in club cells, which are non-ciliated epithelial cells lining both the distal and proximal regions of the human lung epithelium. Additionally, SCGB1A1 expression has been observed in alveolar type 2 progenitor cells, goblet cells, as well as non-mucous and non-ciliated epithelial cells of the human sino-nasal epithelium.[43,44] Under physiological conditions, SCGB1A1 is constitutively produced and is one of the most abundant proteins in the lung.[26] Moreover, SCGB1A1 mRNA has been detected in various epithelial-rich organs, including the uterus, thymus, prostate, and pituitary gland, indicating that SCGB1A1 originating from non-club cells or extrapulmonary tissues may play crucial roles in maintaining homeostasis in organs other than the lung.[28,29] To date, there have been no reports of SCGB1A1 expression in the spleen. Our study demonstrated that SCGB1A1 expression in the spleen of healthy rats is minimal, whereas its expression is significantly elevated in the spleens of COPD model rats. The source of SCGB1A1 in the spleen, an organ lacking typical epithelial cells, remains puzzling. However, studies by Waddell, and others have identified a population of SCGB1A1-expressing cells in the bone marrow of humans and mice, which uniquely coexpress both hematopoietic and mesenchymal markers.[38,45–47] Recent observations in humans undergoing allergen-specific immunotherapy have also shown an upregulation of SCGB1A1 and its mRNA in sputum macrophages and lymphocytes.[48] These findings suggest that under certain conditions, hematopoietic cells, mesenchymal stem cells, macrophages, or lymphocytes in the spleen may have the potential to synthesize and secrete SCGB1A1.

https://doi.org/10.2147/COPD.S506332

It is widely accepted that the anti-inflammatory effects of SCGB1A1 in respiratory diseases are mediated through its ability to bind and sequester key inflammatory mediators, such as prostaglandins, phospholipase A2 (PLA2), and phospholipase C (PLC), and inhibit the activation and translocation of NF-κB.[49–53] However, the immune function of the spleen is primarily carried out by macrophages and lymphocytes, and the immunoregulatory role of SCGB1A1 on these cells has been documented. A recent study showed that exogenous SCGB1A1 supplementation can significantly dampen the response of alveolar macrophages to microbial stimuli, reducing the release of cytokines and chemokines such as IL-1β, IL-6, and IL-8, suggesting a pivotal role of SCGB1A1 in modulating macrophage-mediated inflammation and immune responses.[54] Research by Snyder et al similarly demonstrated elevated TNF-α levels in the airway fluid and cultured lung macrophages of *Scgb1a1*-deficient mice, alongside increased TLR4 expression in these macrophages, indicating that SCGB1A1 attenuates inflammation by modulating macrophage behavior.[55] Regarding lymphocytes, *Scgb1a1*-deficient mice with allergic rhinitis exhibited enhanced T(H)17 responses, while SCGB1A1 treatment significantly reduced these responses.[56] This effect was likely mediated by reduced expression of OX40 ligand, IL-23, and IL-6, and increased CD86 and TGF-β expression in dendritic cells, thus indirectly regulating T(H)17 cell polarization. Additionally, Johansson et al found that SCGB1A1 levels peak early in life and inhibit T(H)2 cell differentiation in infants by modulating dendritic cells, suggesting a critical role for SCGB1A1 in preventing allergic responses during early development.[57] Our cell-based experiments revealed that SCGB1A1 significantly inhibits LPS-induced activation of macrophages in vitro. Additionally, SCGB1A1 effectively suppresses PHA-induced lymphocyte proliferation. However, SCGB1A1 did not exhibit a notable regulatory effect on PHA-induced lymphocyte activation. Given the considerable heterogeneity of macrophage and lymphocyte subsets, as well as the diversity in their activation states and immune functions, our experiments represent only a preliminary exploration. Further comprehensive investigations of SCGB1A1's regulatory effects on splenic immune cells and the underlying molecular mechanisms are required.

Although the findings from this study are intriguing and likely to have significant clinical implications, several limitations must be addressed. For instance, our analysis of SCGB1A1 expression at protein and mRNA levles was confined to splenic tissue, without identifying the specific cellular sources of SCGB1A1. Further studies should employ immunohistochemistry/immunofluorescence staining, or flow cytometry to more accurately determine the distribution and cellular origin of SCGB1A1 within the tissue. Additionally, we have to acknowledge that, due to limitations in experimental resources, we opted for three samples per group in our RNA sequencing experiment. While this sample size may be somewhat limited for this study, it may not be sufficient to capture subtle gene expression differences and biological variability, potentially affecting the robustness and reproducibility of the enrichment analysis results. In future studies, a larger sample size for sequencing analysis may be helpful to further clarify the regulatory mechanisms of splenic function in COPD.

Conclusion

Although the susceptibility of COPD patients to sepsis/septic shock has been widely reported, there is limited research on the functional alterations of the spleen—one of the key organs in the immune response to sepsis—in COPD patients. To our knowledge, this is the first study to investigate the effects of COPD on spleen function at the animal model level using morphological analysis and RNA sequencing techniques. In this study, SCGB1A1 was identified as a critical molecule influencing spleen immune function in COPD, with its regulatory role on macrophages and lymphocytes confirmed in vitro. Given that maintaining physiological levels of SCGB1A1 in the spleen is crucial for optimal steady-state immune function, we speculate that local inhibition of SCGB1A1 in the spleen via gene therapy or monoclonal antibodies around high-risk surgeries or procedures at risk of bloodstream infections in COPD patients might help reduce the incidence of sepsis/septic shock.

Data Sharing Statement

The data that supports the findings of this study are available in the supplementary material of this article.

Ethics Statement

The animal study was reviewed and approved by the Institutional Animal Care and Use Committee at the Medical College of Sun Yat-sen University.

Funding

This study was supported by National Nature Science Foundation of China (No. 81700033, 82071804, 82271813), and Nature Science Foundation of Guangdong Province (No. 2017A030313822, 2022A1515011812).

Disclosure

The authors claim they have no conflicts of interest.

References

1. Agusti A, Celli BR, Criner GJ, et al. Global initiative for chronic obstructive lung disease 2023 report: GOLD executive summary. *Am J Respir Crit Care Med*. 2023;207(7):819–837. doi:10.1164/rccm.202301-0106PP
2. Caramori G, Casolari P, Barczyk A, Durham AL, Di Stefano A, Adcock I. COPD immunopathology. *Semin Immunopathol*. 2016;38(4):497–515. doi:10.1007/s00281-016-0561-5
3. Liu J, Zhang Z, Yang Y, Di T, Wu Y, Bian T. NCOA4-mediated ferroptosis in bronchial epithelial cells promotes macrophage M2 polarization in COPD emphysema. *Int J Chron Obstruct Pulmon Dis*. 2022;17:667–681. doi:10.2147/COPD.S354896
4. Paplinska-Goryca M, Misiukiewicz-Stepien P, Nejman-Gryz P, et al. Epithelial-macrophage-dendritic cell interactions impact alarmins expression in asthma and COPD. *Clin Immunol*. 2020;215:108421. doi:10.1016/j.clim.2020.108421
5. Barnes PJ. Cellular and molecular mechanisms of chronic obstructive pulmonary disease. *Clin Chest Med*. 2014;35(1):71–86. doi:10.1016/j.ccm.2013.10.004
6. Postma DS, Reddel HK, Ten Hacken NH, van den Berge M. Asthma and chronic obstructive pulmonary disease: similarities and differences. *Clin Chest Med*. 2014;35(1):143–156. doi:10.1016/j.ccm.2013.09.010
7. Tanno A, Fujino N, Yamada M, et al. Decreased expression of a phagocytic receptor Siglec-1 on alveolar macrophages in chronic obstructive pulmonary disease. *Respir Res*. 2020;21(1):30. doi:10.1186/s12931-020-1297-2
8. Brusselle G, Bracke K. Targeting immune pathways for therapy in asthma and chronic obstructive pulmonary disease. *Ann Am Thorac Soc*. 2014;11 (Suppl 5):S322–8. doi:10.1513/AnnalsATS.201403-118AW
9. Masubuchi H, Ueno M, Maeno T, et al. Reduced transient receptor potential vanilloid 2 expression in alveolar macrophages causes COPD in mice through impaired phagocytic activity. *BMC Pulm Med*. 2019;19(1):70. doi:10.1186/s12890-019-0821-y
10. Wouters EF, Groenewegen KH, Dentener MA, Vernooy JH. Systemic inflammation in chronic obstructive pulmonary disease: the role of exacerbations. *Proc Am Thorac Soc*. 2007;4(8):626–634. doi:10.1513/pats.200706-071TH
11. Cavailles A, Brinchault-Rabin G, Dixmier A, et al. Comorbidities of COPD. *Eur Respir Rev*. 2013;22(130):454–475. doi:10.1183/09059180.00008612
12. Barbu C, Iordache M, Man MG. Inflammation in COPD: pathogenesis, local and systemic effects. *Rom J Morphol Embryol*. 2011;52(1):21–27.
13. Freeman CM, Martinez CH, Todt JC, et al. Acute exacerbations of chronic obstructive pulmonary disease are associated with decreased CD4+ & CD8+ T cells and increased growth & differentiation factor-15 (GDF-15) in peripheral blood. *Respir Res*. 2015;16(1):94. doi:10.1186/s12931-015-0251-1
14. Cornwell WD, Kim V, Fan X, et al. Activation and polarization of circulating monocytes in severe chronic obstructive pulmonary disease. *BMC Pulm Med*. 2018;18(1):101. doi:10.1186/s12890-018-0664-y
15. Kapellos TS, Bonaguro L, Gemund I, et al. Human monocyte subsets and phenotypes in major chronic inflammatory diseases. *Front Immunol*. 2019;10:2035. doi:10.3389/fimmu.2019.02035
16. Galvis JN, Vargas MV, Robinson HN, et al. Impact of chronic obstructive pulmonary disease on laparoscopic hysterectomy outcome. *JSLS*. 2019;23 (1):e2018.00089. doi:10.4293/JSLS.2018.00089
17. Lee R, Lee D, Mamidi IS, Probasco WV, Heyer JH, Pandarinath R. Patients with chronic obstructive pulmonary disease are at higher risk for pneumonia, septic shock, and blood transfusions after total shoulder arthroplasty. *Clin Orthop Relat Res*. 2019;477(2):416–423. doi:10.1097/CORR.0000000000000531
18. Gu A, Wei C, Maybee CM, Sobrio SA, Abdel MP, Sculco PK. The impact of chronic obstructive pulmonary disease on postoperative outcomes in patients undergoing revision total knee arthroplasty. *J Arthroplasty*. 2018;33(9):2956–2960. doi:10.1016/j.arth.2018.05.009
19. Tahir F, Ahmed J, Malik F. Post-splenectomy sepsis: a review of the literature. *Cureus*. 2020;12(2):e6898. doi:10.7759/cureus.6898
20. Cathomas F, Russo SJ. Brain-spleen connection aids antibody production. *Nature*. 2020;581(7807):142–143. doi:10.1038/d41586-020-01168-0
21. Altamura M, Caradonna L, Amati L, Pellegrino NM, Urgesi G, Miniello S. Splenectomy and sepsis: the role of the spleen in the immune-mediated bacterial clearance. *Immunopharmacol Immunotoxicol*. 2001;23(2):153–161. doi:10.1081/iph-100103856
22. Taniguchi LU, Correia MD, Zampieri FG. Overwhelming post-splenectomy infection: narrative review of the literature. *Surg Infect*. 2014;15 (6):686–693. doi:10.1089/sur.2013.051
23. Torrado C, Baysal MA, Chakraborty A, Norris BL, Khawaja F, Tsimberidou AM. Case report: fatal overwhelming post-splenectomy infection in a patient with metastatic angiosarcoma treated with immunotherapy. *Front Immunol*. 2024;15:1366271. doi:10.3389/fimmu.2024.1366271
24. Abe Y, Itagaki H, Endo T. Overwhelming post-splenectomy infection caused by Escherichia coli 20 years after splenectomy: a case report. *Cureus*. 2023;15(7):e42184. doi:10.7759/cureus.42184
25. Ayenew KD, Ayalew A, Wondmkun YT, et al. In-vivo immunomodulatory activities of essential oils of Artemisia abyssinica and Lepidium sativum in mice. *Immunotargets Ther*. 2024;13:15–27. doi:10.2147/ITT.S448317

26. Martinu T, Todd JL, Gelman AE, Guerra S, Palmer SM. Club cell secretory protein in lung disease: emerging concepts and potential therapeutics. *Annu Rev Med*. 2023;74:427–441. doi:10.1146/annurev-med-042921-123443
27. Klug J, Beier HM, Bernard A, et al. Uteroglobin/Clara cell 10-kDa family of proteins: nomenclature committee report. *Ann N Y Acad Sci*. 2000;923:348–354. doi:10.1111/j.1749-6632.2000.tb05549.x
28. Peri A, Cordella-Miele E, Miele L, Mukherjee AB. Tissue-specific expression of the gene coding for human Clara cell 10-kD protein, a phospholipase A2-inhibitory protein. *J Clin Invest*. 1993;92(5):2099–2109. doi:10.1172/JCI116810
29. Jackson PJ, Turner R, Keen JN, Brooksbank RA, Cooper EH. Purification and partial amino acid sequence of human urine protein 1. Evidence for homology with rabbit uteroglobin. *J Chromatogr*. 1988;452:359–367. doi:10.1016/s0021-9673(01)81460-6
30. Rava M, Tares L, Lavi I, et al. Serum levels of Clara cell secretory protein, asthma, and lung function in the adult general population. *J Allergy Clin Immunol*. 2013;132(1):230–232. doi:10.1016/j.jaci.2013.01.023
31. Guerra S, Halonen M, Vasquez MM, et al. Relation between circulating CC16 concentrations, lung function, and development of chronic obstructive pulmonary disease across the lifespan: a prospective study. *Lancet Respir Med*. 2015;3(8):613–620. doi:10.1016/S2213-2600(15)00196-4
32. Buendia-Roldan I, Ruiz V, Sierra P, et al. Increased expression of CC16 in patients with idiopathic pulmonary fibrosis. *PLoS One*. 2016;11(12): e0168552. doi:10.1371/journal.pone.0168552
33. Tian Y, Li H, Gao Y, et al. Quantitative proteomic characterization of lung tissue in idiopathic pulmonary fibrosis. *Clin Proteomics*. 2019;16:6. doi:10.1186/s12014-019-9226-4
34. Kumar A, Elko E, Bruno SR, et al. Inhibition of PDIA3 in club cells attenuates osteopontin production and lung fibrosis. *Thorax*. 2022;77 (7):669–678. doi:10.1136/thoraxjnl-2021-216882
35. Ye Q, Fujita M, Ouchi H, et al. Serum CC-10 in inflammatory lung diseases. *Respiration*. 2004;71(5):505–510. doi:10.1159/000080636
36. Wendt C, Tram K, Price A, England K, Stiehm A, Panoskaltsis-Mortari A. Club cell secretory protein improves survival in a murine obliterative bronchiolitis model. *Am J Physiol Lung Cell mol Physiol*. 2013;305(9):L642–50. doi:10.1152/ajplung.00021.2013
37. Lopez E, Fujiwara O, Nelson C, et al. Club cell protein, CC10, attenuates acute respiratory distress syndrome induced by smoke inhalation. *Shock*. 2020;53(3):317–326. doi:10.1097/SHK.0000000000001365
38. Bustos ML, Mura M, Hwang D, et al. Depletion of bone marrow CCSP-expressing cells delays airway regeneration. *Mol Ther*. 2015;23 (3):561–569. doi:10.1038/mt.2014.223
39. Zhai J, Insel M, Addison KJ, et al. Club cell secretory protein deficiency leads to altered lung function. *Am J Respir Crit Care Med*. 2019;199 (3):302–312. doi:10.1164/rccm.201807-1345OC
40. Vestbo J, Edwards LD, Scanlon PD, et al. Changes in forced expiratory volume in 1 second over time in COPD. *N Engl J Med*. 2011;365 (13):1184–1192. doi:10.1056/NEJMoa1105482
41. Petersen H, Leng S, Belinsky SA, et al. Low plasma CC16 levels in smokers are associated with a higher risk for chronic bronchitis. *Eur Respir J*. 2015;46(5):1501–1503. doi:10.1183/13993003.00682-2015
42. Knabe L, Petit A, Vernisse C, et al. CCSP counterbalances airway epithelial-driven neutrophilic chemotaxis. *Eur Respir J*. 2019;54(1):1802408. doi:10.1183/13993003.02408-2018
43. Liu Z, Kim J, Sypek JP, et al. Gene expression profiles in human nasal polyp tissues studied by means of DNA microarray. *J Allergy Clin Immunol*. 2004;114(4):783–790. doi:10.1016/j.jaci.2004.04.052
44. Basil MC, Cardenas-Diaz FL, Kathiriya JJ, et al. Human distal airways contain a multipotent secretory cell that can regenerate alveoli. *Nature*. 2022;604(7904):120–126. doi:10.1038/s41586-022-04552-0
45. Bustos ML, Mura M, Marcus P, et al. Bone marrow cells expressing Clara cell secretory protein increase epithelial repair after ablation of pulmonary Clara cells. *Mol Ther*. 2013;21(6):1251–1258. doi:10.1038/mt.2013.53
46. Gilpin SE, Lung K, de Couto GT, et al. Bone marrow-derived progenitor cells in end-stage lung disease patients. *BMC Pulm Med*. 2013;13:48. doi:10.1186/1471-2466-13-48
47. Londhe VA, Maisonet TM, Lopez B, Jeng JM, Li C, Minoo P. A subset of epithelial cells with CCSP promoter activity participates in alveolar development. *Am J Respir Cell mol Biol*. 2011;44(6):804–812. doi:10.1165/rcmb.2009-0429OC
48. Zissler UM, Jakwerth CA, Guerth F, et al. Allergen-specific immunotherapy induces the suppressive secretoglobin 1A1 in cells of the lower airways. *Allergy*. 2021;76(8):2461–2474. doi:10.1111/all.14756
49. Mandal AK, Zhang Z, Ray R, et al. Uteroglobin represses allergen-induced inflammatory response by blocking PGD2 receptor-mediated functions. *J Exp Med*. 2004;199(10):1317–1330. doi:10.1084/jem.20031666
50. Chowdhury B, Mantile-Selvaggi G, Miele L, Cordella-Miele E, Zhang Z, Mukherjee AB. Lys 43 and Asp 46 in alpha-helix 3 of uteroglobin are essential for its phospholipase A2 inhibitory activity. *Biochem Biophys Res Commun*. 2002;295(4):877–883. doi:10.1016/s0006-291x(02)00767-2
51. Okutani R, Itoh Y, Yamada T, et al. Preparation and characterization of human recombinant protein 1/Clara cell M(r) 10,000 protein. *Eur J Clin Chem Clin Biochem*. 1996;34(9):691–696. doi:10.1515/cclm.1996.34.9.691
52. Long XB, Hu S, Wang N, Zhen HT, Cui YH, Liu Z. Clara cell 10-kDa protein gene transfection inhibits NF-kappaB activity in airway epithelial cells. *PLoS One*. 2012;7(4):e35960. doi:10.1371/journal.pone.0035960
53. Pang M, Wang H, Bai JZ, et al. Recombinant rat CC16 protein inhibits LPS-induced MMP-9 expression via NF-kappaB pathway in rat tracheal epithelial cells. *Exp Biol Med*. 2015;240(10):1266–1278. doi:10.1177/1535370215570202
54. Xu M, Yang W, Wang X, Nayak DK. Lung secretoglobin Scgb1a1 influences alveolar macrophage-mediated inflammation and immunity. *Front Immunol*. 2020;11:584310. doi:10.3389/fimmu.2020.584310
55. Snyder JC, Reynolds SD, Hollingsworth JW, Li Z, Kaminski N, Stripp BR. Clara cells attenuate the inflammatory response through regulation of macrophage behavior. *Am J Respir Cell mol Biol*. 2010;42(2):161–171. doi:10.1165/rcmb.2008-0353OC
56. Liu Y, Yu HJ, Wang N, et al. Clara cell 10-kDa protein inhibits T(H)17 responses through modulating dendritic cells in the setting of allergic rhinitis. *J Allergy Clin Immunol*. 2013;131(2):387–94e1–12. doi:10.1016/j.jaci.2012.11.027
57. Johansson S, Wennergren G, Aberg N, Rudin A. Clara cell 16-kd protein downregulates T(H)2 differentiation of human naive neonatal T cells. *J Allergy Clin Immunol*. 2007;120(2):308–314. doi:10.1016/j.jaci.2007.03.021